Effects of CO_2 perturbation on phosphorus pool sizes and uptake in a mesocosm experiment during a low productive summer season in the northern Baltic Sea

M. Nausch[1], L.T. Bach[2], J. Czerny,[2] J. Goldstein[1,a], H.P. Grossart[4,5], D. Hellemann[2,b], T. Hornick[4], E. P. Achterberg[2.3,], K. G. Schulz[2,c], U. Riebesell[2]

[1] {Leibniz Institute for Baltic Sea Research, Seestrasse 15, 18119 Rostock, Germany}

[a] {now at: Max-Planck Odense Center on the Biodemography of Aging & Department of Biology, Campusvej 55, 5230 Odense M, Denmark}

[2] {GEOMAR Helmholtz Centre for Ocean Research Kiel, Düsternbrooker Weg 20, 24105 Kiel, Germany}

[b] {now at: Department of Environmental Sciences, University of Helsinki, PL 65 00014 Helsinki, Finland}

[c] {now at: Centre for Coastal Biogeochemistry, School of Environment, Science and Engineering, Southern Cross University, Lismore, Australia}

[3] {Ocean and Earth Science, University of Southampton National Oceanography Centre Southampton, Southampton SO14 3ZH, United Kingdom}

[4] {Leibniz-Institute for Freshwater Ecology and Inland Fisheries, Zur alten Fischerhütte 2, 16775 Stechlin, Germany}

[5] { Potsdam University, Institute for Biochemistry and Biology, Maulbeerallee 2, 14

469 Potsdam, Germany}

Correspondence to: M. Nausch (monika.nausch@io-warnemuende.de)

Abstract

Studies investigating the effect of increasing CO_2 levels on the phosphorus cycle in natural waters are lacking although phosphorus often controls phytoplankton development in many aquatic systems. The aim of our study was to analyze effects of elevated CO_2 levels on phosphorus pool sizes and uptake. The phosphorus dynamic was followed in a CO_2-manipulation mesocosm experiment in the Storfjärden (western Gulf of Finland, Baltic Sea) in summer 2012 and was also studied in the surrounding fjord water. In all mesocosms as well as in surface waters of Storfjärden, dissolved organic phosphorus (DOP) concentrations of 0.26±0.03 and 0.23±0.04 µmol l^{-1}, respectively, formed the main fraction of the total P-pool (TP), whereas phosphate (PO_4) constituted the lowest fraction with mean concentration of 0.15 ±0.02 µmol l^{-1} in the mesocosms and 0.17±0.07 µmol l^{-1} in the fjord. Transformation of PO_4 into DOP appeared to be the main pathway of PO_4 turnover. About 82% of PO_4 was converted into DOP whereby only 18% of PO_4 was transformed into particulate phosphorus (PP). PO_4 uptake rates measured in the mesocosms ranged between 0.6 and 3.9 nmol l^{-1} h^{-1}. About 86% of them were realized by the size fraction <3 µm. Adenosine triphosphate (ATP) uptake revealed that additional P was supplied from organic compounds accounting for 25-27% of P provided by PO_4 only. CO_2 additions did not cause significant changes in phosphorus (P) pool sizes, DOP composition, and uptake of PO_4 and ATP when the whole study period was taken into account. However, significant short-term effects were observed for PO_4 and PP pool sizes in CO_2 treatments >1000 µatm during periods when phytoplankton biomass increased. In addition, we found significant relationships (e.g., between PP and Chl*a*) in the untreated mesocosms which were not observed under high fCO_2 conditions. Consequently, it can be hypothesized that the relationship between PP formation and phytoplankton growth changed with CO_2 elevation. It can be deduced from the results, that visible effects of CO_2 on P pools are coupled to phytoplankton growth when the transformation of PO_4 into POP was stimulated. The transformation of PO_4 into DOP on the other hand does not seem to be affected. Additionally, there were some indications that cellular mechanisms of P regulation might be changed under CO_2 elevation changing the relationship between cellular constituents.

Kea words

ocean acidification, phosphorus cycling, DOP composition, PO_4 uptake, ATP uptake, Baltic Sea

1. Introduction

Increasing emissions of anthropogenic CO_2 into the atmosphere and subsequent acidification of the ocean can potentially affect the diversity of organisms and the functioning of marine ecosystems (Eisler, 2012). The rise in atmospheric CO_2 concentrations was accelerated from 3.4±0.2 PgC yr^{-1} in the 1980s to 4.0±0.2 PgC yr^{-1} in the 2000s leading to increases of CO_2 in ocean surface waters at a similar rate (IPCC, 2013). Atmospheric CO_2 is projected to rise to 750 - 1000 ppm and higher in 2100 (IPCC, 2001) corresponding with a decrease in open ocean pH by 0.3-0.5 units (Caldeira and Wickett, 2005) from the present level of ~8.1. Although this process is of global significance and all parts of the oceans are at risk, there will be regional differences in the degree of acidification (Borges et al., 2005). Thus, to determine the CO_2-related changes in the oceans, multiple studies in different regions are required. Semi-enclosed coastal regions, such as the Baltic Sea, react with higher changes in pH to CO_2 elevation than open ocean waters due to high freshwater inputs resulting in a reduced buffer capacity (Orr, 2011).

In the Baltic Sea, several studies of CO_2 effects have been undertaken on the organism level of fish (Frommel et al., 2013), zooplankton (Pansch et al., 2012; Vehmaa et al., 2012), macrophytes (Pajusalu et al., 2013), benthic species (Hiebenthal et al., 2013; Stemmer et al., 2013), and filamentous cyanobacteria (Czerny et al., 2009; Eichner et al., 2014; Wannicke et al., 2012). Studies on the impacts of elevated CO_2 at the ecosystem level, however, have thus far been limited to Kiel Bight in the western Baltic Sea (Engel et al., 2014; Rossoll et al., 2013; Schulz and Riebesell, 2013), which may fundamentally differ from other parts of the Baltic Sea.

Next to nitrogen, phosphorus (P) controls the productivity of phytoplankton in the ocean (Karl, 2000; Sanudo-Wilhelmy et al., 2001; Tyrrell, 1999) and is a limiting factor in some regions (Ammerman et al., 2003). The total phosphorus (TP) pool comprises phosphate (PO_4), dissolved organic phosphorus (DOP), and particulate organic (POP) and inorganic (PIP) phosphorus. There is a continuous transformation of phosphorus between these P species due to their uptake, conversion, and release by organisms as well as by interaction with minerals. While PO_4 is the preferred P-species of phyto- and bacterioplankton, DOP can become an important P source when PO_4 is depleted (Llebot et al., 2010; Lomas et al., 2010). DOP includes nucleic acids, phospholipids, and adenosine triphosphate (ATP) (Karl and Björkman, 2002) which are structural and functional components of all living cells, but, can be also released into the surrounding water.

In general, there is little knowledge on how the P cycle is affected by ocean acidification and how related changes in P availability influence the response of organisms to CO_2 elevation. In CO_2 manipulation experiments, particulate phosphorus dynamics were studied to determine

effects on C:P stoichiometry of phytoplankton (Riebesell and Tortell, 2011; Sugie and Yoshimura, 2013) and PO_4 concentration dynamics to estimate its utilization (Bellerby et al., 2008). CO_2 effects on phosphorus pool sizes and PO_4 uptake have so far been studied by Tanaka et al. (2008) in the Raunefjorden, Norway and by Unger et al. (2013) and Endres et al. (2013) in laboratory experiments with cultures of *Nodularia spumigena*. In order to reduce the gap of knowledge, we studied the impact of elevated CO_2 on phosphorus pool sizes, the DOP composition, and PO_4 uptake of a northern Baltic Sea plankton community. These measurements provide important information on potential changes in P cycling under increasing CO_2 levels and contribute to a better understanding of the P cycle in brackish water ecosystems.

2. Material and methods

2.1 Experimental design and CO_2 manipulation

The study was conducted in the northwestern Gulf of Finland, in the proximity of the Tvärminne Zoological Station (TZS) (Fig. 1), between June 17 and August 4, 2012, using the KOSMOS mesocosm system (Riebesell et al., 2013). Nine mesocosms (M1 - M9) were moored in the open waters of the Storfjärden (5951.5 N, 2315.5 E) at a water depth of ~30 m. Only six of them were included throughout the whole study period since leakages in the remaining three rendered them unusable. Equipment and deployment procedures are described in detail by Paul et al. (2015b). Briefly, polyurethane enclosure bags of 2 m in diameter and 18.5 m in length were mounted in floating frames and lowered in such a way that ~17 m of each bag were immersed in the water column and ~1.5 m remained above the water surface. Large organisms were excluded from the mesocosms by a 3-mm mesh installed at the top and bottom of the bags before closure. The mesocosms were deployed 10 days prior to CO_2 manipulation to rinse the bags and for full water exchange. Sediment traps were mounted on the lower ends to close them water tight, while the upper ends were raised above the water surface to prevent water entry during wave action. The mesocosms were covered with a dome shaped roof to prevent nutrient input by bird and potentially significant fresh water input by rain. Salinity gradients were removed by bubbling the mesocosms with compressed air for 3.5 min, so that 5 days before the start of the experiment (day −5) the water body was fully homogeneous.

CO_2 was injected at day 0 and the subsequent 4 days by pumping various quantities of 50-µm-filtered and CO_2-enriched fjord water into seven of the mesocosms as described by Riebesell et al. (2013). The intended CO_2 and pH gradients were reached after the last treatment on day 4. Details are described in Paul et al. (2015b). For the two untreated (control) mesocosms, only

143 filtered fjord water was added to adjust the water volume to that of the treated mesocosms. To
144 compensate for outgassing, the CO_2 manipulation was similarly repeated in the upper 7 m layer
145 of the mesocosms on day 16.
146
147 ## 2.2 Sampling
148 Daily sample collection started 3 days before the first CO_2 injection (day−3). Parallel samples
149 were taken from the surrounding fjord. Sampling over the entire 17 m depth was carried out
150 using an integrating water sampler (IWS HYDROBIOS -KIEL) that was lowered slowly on a
151 cable by hand. The sampling frequency differed depending on the parameter to be observed as
152 shown in the overview by Paul et al. (2015b).
153 Phosphorus pool parameters and uptake rates were determined every second day, except for
154 dissolved organic phosphorus (DOP) components, which were measured every 4 days.
155 Termination of the measurements varied due to logistical constrains. Thus, total phosphorus (TP)
156 and DOP were sampled only until day 29 whereas other parameters were sampled until day 43.
157 The collected water was filled in HCl-cleaned polyethylene canisters that had been pre-rinsed
158 with sample water. All containers were stored in the dark. Back on land, subsamples were
159 processed immediately for each P-analysis. The other analyses were carried out within a few
160 hours of sample collection and sample storage in a climate room at *in situ* temperature.
161
162 ## 2.3 Analytical methods
163 ### 2.3.1 Temperature, salinity, and carbonate chemistry
164 Measurements in the fjord and in each mesocosm were conducted using a CTD60M memory
165 probe (Sea and sun technology, Trappenkamp, Germany) lowered from the surface to a depth of
166 17 m at about 0.3 m s^{-1} in the early afternoon (1:30 - 2:30 pm). For these parameters, depth-
167 integrated mean values are presented here.
168 The carbonate system is described in detail in Paul et al. (2015b). The pHT(total scale) was
169 determined using a spectrophotometric method (Dickson et al., 2007) on a Cary 100 (Varian)
170 and the dye m-cresol as indicator. Extinction was measured at 578 nm (E1) and 434 nm (E2) in a
171 10-cm cuvette. The pH was calculated from the ratio of E1 and E2 (Clayton and Byrne, 1993).
172 DIC was measured using a coulometric AIRICA system (MARIANDA, Kiel) measuring the
173 infrared absorption after N_2 purging of the sample and calibration with certified reference
174 material (CRM; Dr. A. Dickson, University of California, San Diego).
175 The fCO_2 was calculated from DIC, pHT, salinity and using the stoichiometric equilibrium
176 constant for carbonic acid of Mehrbach et al., (1973) as refitted by Lueker et al., (2000).

2.3.2 Chlorophyll and inorganic nutrients

Subsamples of 500 ml were filtered onto GF/F-filters. Chl*a* was extracted in acetone (90 %) in plastic vials by homogenisation of the filters for 5 min. in a cell mill using glass beads. After centrifugation (10 min., 800 x g, 4°C) the supernatant was analysed on a fluorometer (TURNER 10-AU) at an excitation of 450 nm and an emission of 670 nm to determine Chl*a* concentrations (Jeffrey and Welschmeyer, 1997).

A segmented continuous-flow analyzer coupled with a liquid-waveguide capillary flow-cell (LWCC) of 2 m length was used to determine phosphate (PO_4) and the sum of nitrite and nitrate (NO_2+NO_3) at nanomolar precision (Patey et al., 2008). The PO_4 determination was based on the molybdenum blue method of Murphy and Riley (1962), and NO_3+NO_2 on the method of Morris and Riley (1963). PO_4 concentrations from the same subsample were also measured manually using a 5-cm cuvette (Grasshoff et al., 1983). In most of the samplings PO_4 data obtained from both methods did not differ significantly (paired t-test: p=0.262, t=1.127, n=109).

2.3.3 Dissolved organic phosphorus (DOP)

For the determination of DOP, duplicate 40-ml subsamples were filtered through pre-combusted (6 h, 450 °C) glass fiber filters (Whatman GF/F) and stored in 50-ml vials (Falkon) at -20°C until further processing. The thawed samples were oxidized in a microwave (MARS*X*press, CEM, Matthews, USA)(Johnes and Heathwaite, 1992) after the addition of potassium peroxydisulfate in an alkaline medium (Bhaya et al., 2000). The P concentration, measured as PO_4 in a 10-cm cuvette, represents the total dissolved phosphorus (DP) concentration. DOP was calculated as the difference between the DP concentrations in the filtered and digested samples and the corresponding PO_4 concentration analyzed as described above.

2.3.4 Dissolved organic phosphorus compounds

For all analyzed components, subsamples were pre-filtered through pre-combusted (6 h, 450°C) filters (Whatman GF/F) to remove larger particles followed by filtration through 0.2-µm cellulose acetate filters to remove picoplankton. Subsamples were prepared for storage according to the specific method used for each compound. After the analyses, the phosphorus content of measured DOP compounds was summed and the amount subtracted from the total DOP concentration. The difference is defined as the uncharacterized DOP.

Dissolved ATP

The method of (Björkman and Karl, 2001) adapted to Baltic Sea conditions (Unger et al., 2013), was used to determine dissolved adenosine triphosphate (dATP). A $Mg(OH)_2$ precipitate, including the co-precipitated nucleotides, was obtained by treating 200 ml of the filtrate with 2 ml of 1 M NaOH (1% v/v). The precipitate was allowed to settle overnight and then centrifuged at 1000 g for 15 min. The supernatant was discarded and the precipitate was transferred into 50-ml Falcon tubes, centrifuged again (1.5 h, 1680 x g). The resulting pellet was dissolved by drop-wise addition of 5 M HCl. The samples were frozen at -20°C until further processing. The pH of the thawed samples was adjusted to 7.2 by the addition of TRIS buffer (pH 7.4, 20 mM). The final volume was recorded. The dATP concentrations were measured in triplicate using the firefly bioluminescence assay and a Sirius luminometer (Berthold Detection Systems Pforzheim, Germany), as described by Unger et al. (2013). Standard concentrations were prepared as described above, using aged Baltic Sea water and six ATP concentrations (adenosine 50-triphosphate disodium salt hydrate, Sigma-Aldrich, A2383) ranging from 1 to 20 nmol l^{-1}. The detection limit of the bioluminescence assay was 2.5 nmol l^{-1}. The fluorescence slope of the standard concentrations was used to calculate dATP concentrations, correcting for the final sample volume. The P-content of the dATP (dATP-P) was calculated by assuming that 1 mol of ATP is equivalent to 3 mol P.

Dissolved phospholipids

The phosphate content of the dissolved phospholipids (PL-P) was analyzed using a modified method of Suzumura and Ingall (2001, 2004). Briefly, 400-ml subsamples of the filtrate were stored at -20°C until further processing. The samples were then thawed in a water bath at 30°C and extracted twice with 100 ml of chloroform. The chloroform phase was collected, concentrated to 5 ml in a rotary evaporator (Heidolph Instruments, Schwabach, Germany), and then transferred into microwave tubes. The chloroform was completely evaporated by incubating the tubes in a 60°C water bath overnight. After the addition of 20 ml of deionized water (Milli-Q, Millipore), the samples were digested with potassium peroxydisulfate in alkaline medium and microwaved as described for the DOP analysis. Six standard concentrations of phospholipids, ranging from 0 to 125 μg l^{-1}, were prepared by adding the respective amounts of a stock solution containing 5 mg of L-phosphatidyl-DL-glycerol sodium salt (PG, Sigma Aldrich, P8318) ml^{-1} to the aged seawater. The detection limit was 0.8 nmol l^{-1}. The blanks contained only chloroform and were processed as for the samples.

Dissolved DNA and RNA

Dissolved DNA and RNA (dDNA and dRNA) concentrations were determined according to Karl and Bailiff (1989) and as described by Unger et al. (2013). For each sample, 200 ml of the filtrate was gently mixed with the same volume of ethylene-diamine-tetracetic acid (EDTA, 0.1 M, pH 9.3, Merck, 1.08454) and 4 ml of cetyltrimethyl-ammonium bromide (CTAB, Sigma-Aldrich, H5882) and stored frozen at –20°C for at least 24 h. After thawing the samples, the precipitate was collected onto combusted (450°C, 6 h) glass fiber filters (25 mm, GF/F Whatman), placed into annealed vials, and stored frozen at –80°C until further analysis.

DNA concentrations were measured using a fluorescence-spectrophotometer (Hitachi F 2000), and RNA concentrations using a dual-beam UV/VIS-spectrophotometer U3010 (Hitachi).

Coupled standards (DNA + RNA) containing 1–10 µg DNA (Sigma Aldrich, D3779) l^{-1} and 20–120 µg RNA (Sigma Aldrich, R1753) l^{-1} were prepared in aged seawater as described above. A reagent blank served as the reference and aged seawater as the background control. The P-contents of the DNA and RNA were calculated by multiplying the measured values by a factor of 2.06 nmol P per µg dDNA and 2.55 nmol P per µg dRNA. The latter values were determined by the microwave digestion of standard substrates.

2.3.5 Particulate organic phosphorus, carbon, and nitrogen

Particulate phosphorus (PP) was analyzed using two methods in parallel. In the "aqueous method", 40 ml of unfiltered subsamples were frozen at -20°C and analyzed as described for DOP using the potassium peroxydisulfate digestion (Grasshoff et al., 1983). The measured PO_4 concentration represents total phosphorus (TP). PP is the difference between the total PO_4 concentration in the unfiltered digested sample and the sum of DOP+PO_4. In the "filter-method", 500 ml subsamples were filtered onto pre-combusted GF/F-filters that were then placed into Schott bottles containing 40 ml of deionised water. PP was digested to PO_4 by the addition of oxidizing decomposition reagent (Oxisolv®, Merck) followed by heating in a pressure cooker for 30 min. The PO_4 concentrations of the cooled samples were determined spectrophotometrically according to Grasshoff et al. (1983). Paired t-test revealed significant differences between two methods; however, the difference between the means of the filter method and of the aqueous method (0.19 ± 0.03mmol $l^{-1}$and 0.16 ± 0.04µmol l^{-1}, respectively) were near the detection limit (0.02 µmol l^{-1}) of the methods. Thus, solely the mean values obtained from both measurements are used in the following.

Particulate carbon (PC) and nitrogen (PN) were analyzed by filtering 500 ml samples onto pre-combusted (450°C, 6 h) glass fiber filters (Whatman GF/F), which were then stored frozen at -20°C. PC and PN concentrations were measured by flash combustion of the dried (60°C) filters using an EuroEA elemental analyser coupled with a Conflo II interface to a Finnigan Delta^{Plus} mass spectrometer and include organic and inorganic matter.

2.3.6 Phosphate and ATP uptake

PO_4 uptake was measured by addition of radioactively labeled phosphate [^{33}P]PO_4 (specific activity of 111 TBq mmol^{-1}, Hartmann Analytic GmbH) at concentrations of 50 pmol l^{-1} to 50 ml subsamples, which were then incubated under laboratory light and the *in situ* temperatures for ~2 h. For each mesocosm, three parallel samples and a blank were prepared. The blank was obtained by the addition of formaldehyde (1% final concentration) 10 min before radiotracer addition, in order to poison the samples. At defined time intervals within the incubation, 5-ml subsamples were taken from each of the parallel samples and filtered onto polycarbonate (PC) filters pre-soaked with a cold 20 mM PO_4 solution to prevent non-specific [^{33}P]PO_4 binding. The filters were rinsed with 5 times 1 ml of particle-free bay water and placed in 6-ml scintillation vials. Scintillation liquid (4 ml IrgaSafe; Perkin Elmer) was added and the contents of the vials were mixed using a vortex mixer. After allowing the samples to stand for at least 2 h, the radioactivity on the filters was counted in a Perkin Elmer scintillation counter. PC-filters of 0.2 µm and 3 µm pore sizes (Whatman and Millipore, respectively) were used to determine uptake by the whole plankton community and the size fraction >3µm, respectively. Picoplankton uptake was calculated as the difference between the activity on the 0.2-µm and 3-µm filters.

[γ^{33}P]ATP (specific activity of 111 TBq mmol^{-1}, Hartmann Analytic GmbH) was added to triplicate 10-ml samples and a blank, each in a 20-ml vial, at a concentration of 50 pmol l^{-1}. The samples were incubated in the dark at the *in situ* temperature for 1 h. The uptake was stopped by addition of 200 µl of a cold 20 mM ATP solution to the samples, which were then filtered and processed as described for the PO_4 uptake measurements.

2.3.7 Bacterial production (BPP)

Rates of bacterial protein production (BPP) were determined by incorporation of ^{14}[C]-leucine (^{14}C-Leu, Simon and Azam, 1989) according to Grossart et al. (2006). Triplicates and a formalin-killed control were incubated with ^{14}C-Leu (7.9 GBq mmol^{-1}; Hartmann Analytic GmbH, Germany) at a final concentration of 165 nmol l^{-1}, which ensured saturation of uptake

systems of both free and particle-associated bacteria. Incubation was performed in the dark at *in situ* temperature (between 7.8°C and 15.8°C) for 1.5 h. After fixation with 2% formalin, samples were filtered onto 5.0 µm (attached) nitrocellulose filters (Sartorius, Germany) and extracted with ice-cold 5% trichloroacetic acid (TCA) for 5 min. Thereafter, filters were rinsed twice with ice-cold 5% TCA, once with ethanol (96% v/v), and dissolved with ethylacetate for measurement by liquid scintillation counting. Afterwards the collected filtrate was filtered on 0.2 µm (free-living) nitrocellulose filters (Sartorius, Germany) and processed in the same way as the 5.0 µm filters. Standard deviation of triplicate measurements was usually <15%. The sum of both fractions (free-living bacteria and attached bacteria) is referred to total BPP. The amount of incorporated ^{14}C-Leu was converted into BPP by using an intracellular isotope dilution factor of 2 (Simon and Rosenstock, 1992). A conversion factor of 0.86 was used to convert the protein produced into carbon (Simon and Azam, 1989).

2.4 Statistical analyses

The Grubbs test, done online (graphpad.com/quickcalcs/Grubbs1.cfm) was applied to identify outliers in all data sets. The outliers were removed from further statistical analyses.

Spearman Rank correlations were carried out to describe the relationship between the development of the parameters over time in the mesocosms and in the fjord using Statistica 6 software.

Short-term CO_2 effects on PP concentrations at days 0-2 and 23-43 between the CO_2 treatments were verified with an ANCOVA analysis using the SPSS software. The "days" were treated as a covariate interacting with the treatments. Paired t-test was applied to check the differences in PO_4 concentrations between the treatments.

3. Results

3.1 Development in the mesocosms

3.1.1 CO_2, pH, temperature and salinity

The different mesocosms were characterized based on their averaged fCO_2 and pH values from day 1 until day 43 (Fig.2a, b):

M1 365 µatm fCO_2, pH 8.08

M5 368 µatm fCO_2. pH 8.07

M7 497 µatm fCO_2, pH 7.95

M6 821 µatm fCO_2, pH 7.74

M3 1007 µatm fCO_2, pH 7.66

M8 1231 µatm fCO_2, pH 7.58

M1 and M5 were the untreated mesocosms and served as controls.

Temperature development in the mesocosms closely followed that in the fjord ranging from 7.82°C to 15.86°C. Based on this (compare Paul et al. 2015b for details), the experiment was divided into four phases (Fig. 3): phase 0: day -3 to day 0; phase I: days 1–16, phase II: days 17–30 and phase III: day 31 until the end of the measurements. Temperature dropped from 8.71°C to 7.82°C in phase 0 and rose from 8.07°C at the start of phase I to the maximum of 15.86°C by the end of this phase. During phase II, the temperature decreased to 7.89°C interrupted by a short reversal on days 22 and 23. During phase III, the temperature increased to 12.61°C (Table 1).

Salinity (5.69±0.01) remained relatively stable in all mesocosms throughout the entire experimental period (Fig. 3).

3.1.2 Phytoplankton biomass

Chlorophyll *a* (Chl*a*) reached maximum concentrations of 2.06–2.48 µg l^{-1} at day 5 (Fig. 4). Average concentrations of 1.94±0.23 µg l^{-1} in phase I exceeded those in phases II and III when Chl*a* decreased to a mean of 1.08±0.16 µg l^{-1}. The increase in Chl*a* in the high CO_2 mesocosms by 0.27µg l^{-1} in phase III was marginal for Baltic Sea summer conditions. According to Paul et al. (2015b), this represents an increase of 24% which is a significant difference compared to the controls.

We observed a significant relationship between Chl*a* and PO_4 in the untreated and intermediate treated mesocosms that diminished with increasing fCO_2 as indicated by lower p-values. The statistical significance was lost in the highest fCO_2 mesocosms (Table 2).

3.1.3 Phosphorus Pools

Total phosphorus (TP) concentrations in the mesocosms ranged between 0.49 and 0.68 µmol l^{-1} (Fig. 5a) during the experiment without statistically significant differences between the CO_2 treatments. Shortly after the bags were closed, the decline in TP concentrations began and continued until the beginning of phase II. On average, TP concentrations decreased from 0.63±0.02 µmol l^{-1} on day −3 to 0.51±0.01 µmol l^{-1} on day 21. Thereafter, the mean TP remained constant at 0.54±0.03 µmol l^{-1} until the end of the measurements. Thus, the loss of phosphorus (116 ± 34 nmol l^{-1}) from the 17-m layer during the 29-day measurement period was calculated to be 4.0 nmol l^{-1} day^{-1}. The decline in TP can be explained by loss through sedimentation of PP (Paul et al., 2015b).

Particulate phosphorus (PP) concentrations varied from 0.10 to 0.23 µmol l^{-1} in all CO_2 treatments (Fig. 5b, Fig. 6). We expected that the decrease in TP was reflected in PP. However, parallel changes occurred only periodically. PP concentrations increased during the first 5 days after the bags were closed. This increase was stimulated by CO_2 additions from day 0 to day 2 (ANCOVA: p=0.004, F=20.811) (Fig. 7a). Subsequently, PP declined in parallel with TP until day 21, albeit with a lower amount. Averaged over all mesocosms, TP decreased by 0.12 ± 0.03 µmol l^{-1}, whereas PP declined only by 0.06 ± 0.01 µmol l^{-1} during this period. From day 23 until the end of the measurements, PP remained at relatively constant concentrations; however, PP concentrations in the high CO_2 treated mesocosms exceeded those in the other mesocosms significantly (ANCOVA: p<0.0001, F=11.99) (Figs. 5b, 7). PP developed in parallel with PC. The two parameters were positively correlated in the untreated and the intermediate CO_2 treatments, but not in the high CO_2 treatments (Table 2). Figures 3 and 6b show that the increase in Chl*a* was delayed by 2–3 days compared to the increase in PP during the first growth event. A correlation between PP and Chl*a* was detected only for the untreated mesocosms (Table 2).

Dissolved organic phosphorus (DOP) concentrations in the mesocosms ranged between 0.18 and 0.36 µmol l^{-1} constituting 32–71% of the TP pool (Fig. 5c). DOP did not change significantly in response to the CO_2 perturbations, and were similar to the concentrations in fjord water. Concentrations of ≥0.3 µmol l^{-1} were measured on days 6 and 7 (phase I) and on day 23 (phase II); the high DOP value in the intermediate CO_2 treatment at day 19 was identified as an outlier according to Grubbs test (Fig. 5c).

In phase I, DOP initially increased in parallel with Chl*a* and BPP but reached its maximum 1–2 days later, after which it decreased only marginally until the end of this phase, independent of changes in BPP and Chl*a* (Fig. 8c, d). In phase II, the peak conformed to that of BPP. DOP correlated with temperature only in the high fCO_2 mesocosms (Table 2). In addition, the composition of DOP did not change with increasing CO_2 (Fig.10). The sum of RNA (~47%) plus the unidentified fraction constituted 98–99% of the DOP pool whereas the other measured compounds contributed only 1–2% (Table 3).

Phosphate (PO_4) concentrations ranged between 0.06 and 0.21 µmol l^{-1}, with deviations between the mesocosms only in nanomolar range. The mean contribution of PO_4 to TP was 25±6%, which was the lowest among all TP fractions (Fig. 6). From the start of the measurements to day 13, PO_4 declined by 0.06 µmol l^{-1} (or 3.5 nmol l^{-1} day^{-1}) from initial

values of 0.16±0.01 µmol l^{-1} (Fig. 5d). Subsequently, concentrations increased again, by an average of 2.6 nmol l^{-1} day^{-1}, until the end of the experiment. There were no significant differences between CO_2 treatments until day 23, when high CO_2 concentrations led to slightly lower PO_4 concentrations (Fig. 5d). Afterwards, PO_4 concentrations in the high fCO_2 mesocosms were significantly lower than those in the untreated mesocosms (t=6.51, p=0.0003). This observation is in accordance with the dynamics of PP and Chl*a* concentrations, which were significantly elevated in the high CO_2 treatments. Thus, the transformation of PO_4 to POP via stimulated biomass formation may have been promoted under high CO_2 conditions in phase III. Since PO_4 was never fully exhausted, phosphorus limitation of phyto- and bacterioplankton can be excluded. This interpretation is supported by the PC:PP ratios, which varied between 84.4 and 161.1 in all treatments (Paul et al.,2015b) deviating only slightly from the Redfield ratio.

3.1.4 Uptake of PO_4 and ATP

PO_4 turnover times of 1.5–8.4 days (mean 4.0±1.2 days, n= 112) in all mesocosms indicated no dependency on the CO_2 treatment (Fig. 9a). Gross PO_4 uptake rates were in the range of 0.6–3.9 nmol l^{-1} h^{-1} (mean 1.7±0.6 nmol l^{-1} h^{-1}, n=112), or 14.3–94.4 nmol l^{-1} day^{-1} (mean 41.3±13.8 nmol l^{-1} day^{-1}) (Fig. 9b, Table 4). The rates were highest on days 4 and 9 (phase I) and decreased thereafter until day 15, followed by an increase to a mean maximum rate of 2.3±0. 5 nmol l^{-1} h^{-1} (n=6) at day 27. The size fraction <3 µm was responsible for 59.1 to 98.4% of the total PO_4 uptake (mean 86.5±7.6%) whereas the size fraction >3 µm accounted for only 1.6–40.9% (mean 13.5±7.4%). Thus, PO_4 was taken up mainly by picoplankton. However, only the uptake rate by the size fraction >3 µm was positively related to Chl*a* and inversely related to the P content of the biomass (Table 2). Thus the PO_4 uptake was obviously stimulated when the phytoplankton biomass increased and at simultaneous decrease of the cellular P. The relationship between PO_4 uptake by this fraction and Chl*a* became evident only in the CO_2-amended conditions indicating that the interaction between P uptake, cellular P-content and growth of phytoplankton was stimulated under elevated CO_2 conditions.

ATP turnover times of 0.2 to 3.6 days (mean 0.94±0.74 days, n=90) were much shorter than the PO_4 turnover times and did not vary between the treatments (Fig. 9c). Between 0.05 and 0.36 nmol ATP l^{-1} h^{-1} (mean 0.14±0.08 nmol l^{-1} h^{-1}, n=36) were hydrolysed, corresponding to a P supply of 0.14 and 1.08 nmol l^{-1} h^{-1} (mean 0.44±0.25 nmol l^{-1} h^{-1}, n=36). Thus, phosphorus additionally supplied from ATP accounted for ~25% of that provided by PO_4. The picoplankton size fraction (<3 µm) was responsible for 90–99% of ATP uptake, with only a marginal portion (1.6–9.5%) attributable to the phytoplankton fraction >3 µm (Table 4).

448

449 ### 3.2 Hydrography and pool sizes in the fjord

450 Large variations in fCO_2 and pH occurred in fjord water during the period of investigation (Table
451 1). The relationship of fCO_2 with temperature and salinity indicated that the CO_2 conditions were
452 influenced predominantly by changes in the water masses, specifically by upwelling which
453 affected both the relationship of fCO_2 with PO_4 and probably the correlation of fCO_2 with Chl*a*
454 and PC (Table 2). fCO_2 ranged from 207 µatm (Fig. 2a) at days 12-16 when temperatures were
455 highest to 800 µatm at day 33 when deep water input occurred which was indicated by pH below
456 7.75.

457

458 **Chl*a*** concentrations were between 1.12 and 5.46 µg l^{-1} (mean 2.29 ± 1.11 µg l^{-1}; n=38), with
459 distinct phases correlating with temperature, salinity and pH. However, the Chl*a* maximum
460 occurred at the beginning of phase II, which was 1-2 days after the maximum temperature.
461 Shortly thereafter, Chl*a* decreased to its lowest level before it increased again, albeit only
462 marginally to 1.93 µg l^{-1} during phase III (Fig. 4).

463

464 **TP** concentrations from day -3 until day 29 ranged between 0.54 and 0.70 µmol l^{-1} (mean
465 0.61±0.04 µmol l^{-1}; n=19) (Figs. 5a, 6). With a general decreasing tendency, TP undulated with
466 a frequency of about 10 days in the period of phases 0 to the first half of phase I and of 6 days in
467 the second half of phase I to II. For the period under investigation, the TP fractions had the
468 following characteristics:

469 **PP** concentrations varied from 0.13 to 0.30 µmol l^{-1} (mean 0.20±0.04 µmol l^{-1}; n=29), thus
470 accounting for 23.4–51.8% (mean 34.7±7.9%; n=19) of the TP pool. The development of PP
471 over time did not follow that of TP (Fig. 5b). PP concentrations were highest between days 8 and
472 19, when the accumulation of PP in the biomass was reflected in declining C:P ratios from 180
473 to 107 (Paul et al. 2015b) and thereafter remained at the low ratio until the end of the
474 measurements. The PP increase in phase III occurred in parallel to Chl*a* and to the PO_4 decrease
475 (Fig. 6). Thus PO_4 was transformed into PP via biomass production. The calculated P content of
476 phytoplankton was 0.05–0.15 (mean 0.1) µmol PP (µg Chl*a*)$^{-1}$.

477 **DOP** substantially contributed (26–45%) to the TP pool (Fig. 6). Concentrations ranged between
478 0.19 and 0.29 µmol l^{-1} (mean 0.24±0.03 µmol l^{-1}; n=17), with high concentrations occurring in
479 parallel to those of TP in phases I and II (Fig. 5c). The very low DOP value of 0.11 µmol l^{-1}, on
480 day 29, was an outlier (Grubbs test). For the whole study period, DOP concentrations correlated
481 positively with PP (p= 0.034, n=17) and inversely with PO_4 concentrations (p=0.005, n=17). A

similar behavior between DOP and Chl*a* was restricted to phases 0 and I, whereas the relationship was inverse in phase II (Fig. 8b). As shown in Figure 8a, the DOP and BPP levels alternated with the same rhythm, but inversely, in phases 0 and I and changed to a parallel development in phase II. Statistical analysis was not feasible because DOP and BPP were not always sampled on the same day and only very few data pairs were available.

PO_4 concentrations ranged between 0.06 and 0.41 µmol l^{-1} (mean 0.21±0.09 µmol l^{-1}, n=21), thus comprising 24.3±11.2% (n=21) of the TP pool (Fig. 6). With a few exceptions, PO_4 concentrations declined from the beginning of the study period until the end of phase I and increased during phase II and the beginning of phase III. These changes were caused by upwelling of PO_4 enriched deep water of higher salinity and lower temperatures. The subsequent decline in PO_4 between days 33 and 40 was caused by the stimulation of phytoplankton production, as indicated by the increase in Chl*a* concentration (Fig. 4).

4. Discussion

An increase in CO_2 in marine waters and the associated acidification may potentially have multiple effects on organisms and biogeochemical element cycling (Gattuso and Hansson, 2011). Reported findings indicate wide ranging responses, probably depending on the investigated species and growth conditions. For example, CO_2 stimulation as well as lack of stimulation were found for primary production and carbon fixation (Beardall et al., 2009; Boettjer et al., 2014), DOC release (Engel et al., 2014; MacGilchrist et al., 2014) and phytoplankton growth (Riebesell and Tortell, 2011). An interaction of CO_2 effects with phosphorus and iron availability has been found by Sun et al. (2011) for a the diatom *Pseudo-nitzschia multiseries* and by Yoshimura et al. (2014) for a diatom dominated subarctic plankton community. Thus, responses of organisms and ecosystems to enhanced CO_2 concentrations are complex and still poorly understood. The present study is the first to determine the effects of increased CO_2 levels on phosphorus cycling in a brackish water ecosystem.

4.1 Response of P-pools and P-uptake to enhanced CO_2 in the mesocosms

The Finish coast of the Gulf of Finland is one of the most important upwelling regions in the Baltic Sea. During our investigation in 2012, surface temperatures, obtained from the NOAA satellite (Siegel and Gerth, 2013) showed that upwelling persisted during the whole study period but with varying intensity. The intensity of upwelling shaped the pattern of temperature not only

in the fjord but also in the mesocosms varying from 7.8 to15.9°C. Such variations in temperature influence the phosphorus transformation and interleave with CO_2 effects.

While nutrients were added in previous CO_2 enrichment experiments (Riebesell et al., 2008; 2013; Schulz et al., 2008), no amendments were undertaken in this study in order to be close to natural conditions. Initial PO_4 concentrations of only 0.17 ± 0.01 µmol l^{-1} were measured, however, PO_4 was never exhausted (Figs. 5, 6). Cellular C:P and N:P ratios were close to the Redfield ratio. Therefore, phosphorus limitation unlikely occurred in this experiment. Simultaneous low nitrate and ammonium concentrations (Paul et al. 2015b) formed nutrient conditions that benefit the growth of diazotrophic cyanobacteria. However, a cyanobacteria bloom failed to appear, despite the low-level presence of *Aphanizomenon* sp. and *Dolichospermum* sp. (Paul et al., 2015a) as potential seed stock. For Baltic Sea summer conditions, the phytoplankton development with maximum Chl*a* concentrations of 2.2–2.5 µg l^{-1} remained relatively low with the highest contribution of cryptophytes and chlorophytes in phase I and at the beginning of phase II. Picoplankton was mostly the dominating size fraction, amounting ~20-70% of Chl*a* in phase I and up to ~85% in phase III (Paul et al., 2015b). However, a positive correlation of fCO_2 with Chl*a* was observed only for the size fraction >20 µm. The abundance of diatoms that could be a part of this fraction increased from ~day 23 to day 30 and might have an influence on this relationship.

Against this background, the CO_2 perturbation did not cause significant changes in phosphorus pool sizes, DOP composition, and P-uptake rates from PO_4 and ATP when the whole study period was considered. However, small but yet significant short-term effects on PO_4 and PP pool sizes were observed in phases I, III and partially in phase II (Fig. 7). CO_2 elevation stimulated the formation of PP until day 3 (Fig. 5b) when chlorophytes, cyanobacteria, prasinophytes and the pico-cyanobacteria started to grow (Paul et al., 2015b).

The effects of CO_2 addition on PO_4 and PP pool sizes were evident from day 23 onwards (Figs. 5b, 7). PO_4 concentrations were slightly, but significantly lower in the high CO_2 treatment than in the untreated mesocosms, accompanied by significantly elevated PP concentrations. This indicates that the transformation of PO_4 into PP was likely stimulated under high CO_2 conditions. Since Chl*a* was also elevated at similar PP:Chl*a* ratios, the PO_4 taken up was used for new biomass formation. However, the elevated transformation of PO_4 into PP was not reflected in the PO_4 uptake rates which can be seen as gross uptake rates. But, an increase of PP, caused by biomass formation, while the PO_4 uptake remained unchanged can only occur when the P release from organisms is reduced. Thus, it is likely that not the gross uptake but rather the net uptake was modified under CO_2 elevation.

While in phases II and III, high CO_2 levels caused a change in the PP and PO_4 pools for about 22 days, changes lasting only 2 days have been observed at the beginning of phase I (Fig.7a), but, shorter effects cannot be excluded. Uptake and release are assumed to be continuous processes and can alter the P pool sizes on timescales shorter than one day. Thus, variations and differences in the treatments can be overseen at daily sampling. Unger et al. (2013) demonstrated that an accelerated PO_4 uptake by the cyanobacterium *Nodularia spumigena* under elevated CO_2 incubations could only be observed during the first hours. Thereafter, the differences were balanced and the same level of radiotracer labeling was reached in all treatments. An acceleration in the formation of particulate P under CO_2 elevation without any changes of PO_4 turnover times was also observed by Tanaka et al. (2008). They observed an increase of the PP amount and an earlier appearance of the PP maximum under CO_2 elevation.

Correlations calculated by using the Spearman rank test between P pools or uptake rates and other parameters for each mesocosm are presented in Table 2. The relationships between PP and TP with Chl*a* disappeared at elevated fCO_2, whereas correlations developed between PP and PC as well as between the PO_4 uptake by phytoplankton in the >3 µm size class and the PP:Chl*a* ratio (Table 2). These shifts could be caused by changes in the phytoplankton composition deduced from CO_2 effects on the pigment composition (Paul et al., 2015b).

Independent of the CO_2 treatment, TP decreased by 2.6 nmol l^{-1} day^{-1} in all mesocosms over the course of the experiment, in agreement with the measured sedimentation rates (Paul et al., 2015b). The strongest decrease (~3.2 nmol l^{-1} day^{-1}) occurred during phase I. Of the total TP removal during this phase (48 nmol l^{-1}), 84% (~40.5 nmol l^{-1}) could be explained by the decrease in PP and 16% (~ 8 nmol l^{-1}) by changes in the dissolved pool. However, the PO_4 decline (~34.5 nmol l^{-1}) was stronger than that of the total dissolved P pool since DOP increased in parallel by ~26.5 nmol l^{-1}. Thus, about 77% of the PO_4 reduction was retrieved as DOP and remained in the dissolved P-pool as the main pathway of PO_4 transformation.

4.2 Phosphorus dynamics in the Storfjärden

Nutrients in upwelled water during our study were depleted in dissolved inorganic nitrogen and enriched in PO_4, as reported for other upwelling areas of the Baltic Sea (Lass et al., 2010). Thus, ammonium and NO_2+NO_3 concentrations in the surface water were only in the nanomolar range (Paul et al., 2015b). PO_4 increased in parallel with the increase in salinity and decrease in temperature. Maximum PO_4 concentrations of 0.33 µmol l^{-1} and 0.42 µmol l^{-1} (Figs 5, 6) were observed at the end of the upwelling events in phases 0 and II, respectively. The correlation with

583 Chl*a* and PP indicated that PO_4 was utilized during plankton growth in the subsequent relaxation
584 phases I and III. Due to PO_4 input into surface water, the phytoplankton community was unlikely
585 P-limited indicated by PC:PP ratios of 86–189 (mean 125, n=23) (Paul et al., 2015b). However,
586 the PO_4 availability might be not the only reason for the good P-nutritional status of the
587 plankton. It can be deduced from the long PO_4 turnover times in the mesocosms, where external
588 input was excluded, that the P demand of the plankton community might be low. The P content
589 deduced from PP:Chl*a* ratios of 0.05–0.15 µmol P (µg Chl*a*)$^{-1}$ was somewhat lower than those
590 observed during an upwelling event along the east coast of Gotland, where ratios between 0.1
591 and 0.2 µmol P (µg Chl*a*)$^{-1}$ (Nausch et al., 2009) were estimated.
592 PP concentrations of 0.13–0.3 µmol l^{-1} were in the range typically observed in the Baltic Proper
593 (Nausch et al., 2009; Nausch et al., 2012). However, PP concentrations in the Gulf of Finland
594 may reach higher values, as was the case in the summer of 2008, when the observed PP
595 concentration was 0.35 ± 0.07 µmol l^{-1} (Nausch and Nausch, 2011).
596 DOP concentration of 0.27 ± 0.02 µmol l^{-1} during our study was similar to that detected in the
597 Gulf of Finland in the summer of 2008 (Nausch and Nausch, 2011). In the Baltic Sea, DOP
598 exhibits vertical gradients with maximum concentrations in the euphotic surface layer and lower
599 than 0.1 µmol l^{-1} at depths below 25 m. Thus, the observed DOP dynamics in surface water
600 during our study can be assumed to be the result of release, consumption and mineralization by
601 organisms or input from land. The relationship of DOP with Chl*a* and BPP (Fig. 8) indicated that
602 the increased DOP concentrations in phase I may be due to release by phytoplankton
603 supplemented by bacterial release. DOP can be accumulated in water only when the release
604 exceeded the consumption or degradation. During phase II, phytoplankton biomass was low and
605 DOP release should thus be minor. Since the small mesozooplankton increased in the fjord
606 similar to those reported for the mesocosms in phases II and III (Paul et al. 2015b) DOP could be
607 released during grazing combined with the observed temporal offset of BPP and DOP maxima.
608 Thus, the observed DOP variations may be the result of processes in the surface water.
609
610
611 ## 5. Conclusions
612 Surface water in Storfjärden showed highly variable fCO_2 conditions and reached levels of up to
613 800 µatm, which is similar to that expected in ca. 100 years from now. Deduced from the high
614 frequency of upwelling events, organisms experience elevated fCO_2 more or less regularly. Thus,
615 a general impact of fCO_2 on P pools and P uptake rates in the mesocosms could not be identified
616 for the overall period of investigation. However, short-term responses to fCO_2 elevation lasting

only few days were observed for the transformation of PO_4 into PP that was linked with stimulation of phytoplankton growth. Although statistically significant, it is difficult to assess if the differences between the treatments are of ecological relevance. Such short-term variations are possible in the phosphorus dynamics since the pools size can be transformed within hours and there changes are in the nanomolar concentration range. There are also indications that relationships of P pool sizes or uptake with Chl*a* and PC can change as fCO_2 increases, but the underlying mechanisms are still unclear. The transformation of PO_4 into DOP was not affected by CO_2 elevation. It may be the major pathway of phosphorus cycling under hydrographical and phytoplankton growth conditions as occurred in our experiment.

Acknowledgement

We are grateful to the KOSMOS team for their invaluable help with the logistics and maintenance of the mesocosms throughout the experiment. In particular, we sincerely thank Andrea Ludwig for organizing and coordinating the campaign and for the daily CTD measurements. We appreciate the assistance of Jehane Ouriqua in the nutrient analysis and that of many other participants who carried out the samplings. We also appreciate the collegial atmosphere during the work and thank everyone who contributed to it. We would also like to acknowledge the staff of the Tvärminne Zoological Station for their hospitality and support, for allowing us to use the experimental facilities, and for providing CTD data for the summers of 2008–20011. Finally, we thank Jana Woelk for analysing the phosphorus samples in the IOW. This study was funded by the BMBF project BIOACID II (FKZ 03F06550).

References

Ammerman, J. W., Hood, R. R., Case, D., and Cotner, J. B.: Ph

osphorus deficiency in the Atlantic: an emerging paradigm in oceanography, Eos (Washington DC), 84, 165–170, 2003.

Beardall, J., Stojkovic, S., and Larsen, S.: Living in a high CO2 world: impacts of global climate change on marine phytoplankton, Plant. Ecol. Divers., 2, 191-205, 2009.

Bellerby, R. G. J., Schulz, K. G., Riebesell, U., Neill, C., Nondal, G., Heegaard, E., Johannessen, T., and Brown, K. R.: Marine ecosystem community carbon and nutrient uptake stoichiometry under varying ocean acidification during the PeECE III experiment, Biogeosciences, 5, 1517-1527, 2008.

651 Bhaya, D., Schwarz, R., and Grossman, A. R.: Molecular Response to environmental stress. in: Whitton.,
652 B.A. and Potts, M,(eds) The Ecology of Cyanobacteria 2000. 397-442., 2000.

653
654 Björkman, K. M. and Karl, D. M.: A novel method for the measurement of dissolved adenosine and
655 guanosine triphosphate in aquatic habitats: applications to marine microbial ecology, J Microbiol.
656 Methods, 47, 159-167, 2001.

657
658 Boettjer, D., Karl, D. M., Letelier, R. M., Viviani, D. A., and Church, M. J.: Experimental assessment of
659 diazotroph responses to elevated seawater pCO(2) in the North Pacific Subtropical Gyre, Glob.
660 Biogeochem. Cycle, 28, 601-616, 2014.

661
662 Borges, A. V., Delille, B., and Frankignoulle, M.: Budgeting sinks and sources of CO2 in the coastal ocean:
663 Diversity of ecosystems counts, Geophys. Res. Lett., 32, 1-4, 2005.

664
665 Caldeira, K. and Wickett, M. E.: Ocean model predictions of chemistry changes from carbon dioxide
666 emissions to the atmosphere and ocean, J. Geophys. Res.-Oceans, 110, 1-12, 2005.

667
668 Clayton, T. D. and Byrne, R. H.: Spectrophotometric seawater pH measurements: total hydrogen ion
669 concentration scale calibration of m-cresol purple and at-sea results, Deep-Sea Res. Part I-Oceanogr.
670 Res. Pap., 40, 2115–2129, 1993.

671
672 Czerny, J., Ramos, J. B. E., and Riebesell, U.: Influence of elevated CO2 concentrations on cell division
673 and nitrogen fixation rates in the bloom-forming cyanobacterium Nodularia spumigena, Biogeosciences,
674 6, 1865-1875, 2009.

675
676 Dickson, A. G., Sabine, C. L., and Christian, J. R.: Guide to best practices for ocean CO2 measurements,
677 North Pacific Marine Science Organization, (PICES Special Publication, 3) Sidney, BC, Canada. 191pp.
678 http://aquaticcommons.org/1443/, 2007.

679
680 Eichner, M., Rost, B., and Kranz, S. A.: Diversity of ocean acidification effects on marine N-2 fixers, J. Exp.
681 Mar. Biol. Ecol., 457, 199-207, 2014.

682
683 Eisler, R.: Ocean Acidification. A comprehensive overview, Science Publisher, St. Helier, Jersey, British
684 Channel Islands. 252pp., 2012.

685
686 Endres, S., Unger, J., Wannicke, N., Nausch, M., Voss, M., and Engel, A.: Response of Nodularia
687 spumigena to pCO(2) - Part 2: Exudation and extracellular enzyme activities, Biogeosciences, 10, 567-
688 582, 2013.

689
690 Engel, A., Piontek, J., Grossart, H. P., Riebesell, U., Schulz, K. G., and Sperling, M.: Impact of CO2
691 enrichment on organic matter dynamics during nutrient induced coastal phytoplankton blooms, J.
692 Plankton Res., 36, 641-657, 2014.

693

694 Frommel, A. Y., Schubert, A., Piatkowski, U., and Clemmesen, C.: Egg and early larval stages of Baltic cod,
695 Gadus morhua, are robust to high levels of ocean acidification, Mar. Biol., 160, 1825-1834, 2013.

696
697 Gattuso, J. P. and Hansson, L.: Ocean acidification, Oxford University Press, Oxford, 326pp, 2011.

698
699 Grasshoff, K., Ehrhardt, M., and Kremling, K. (Eds.): Methods of seawater analysis, Verlag Chemie,
700 Weinheim, 419 pp., 1983.

701
702 Grossart, H. P., Allgaier, M., Passow, U., and Riebesell, U.: Testing the effect of CO2 concentration on the
703 dynamics of marine heterotrophic bacterioplankton, Limnol. Oceanogr., 51, 1-11, 2006.

704
705 Hiebenthal, C., Philipp, E. E. R., Eisenhauer, A., and Wahl, M.: Effects of seawater pCO(2) and
706 temperature on shell growth, shell stability, condition and cellular stress of Western Baltic Sea Mytilus
707 edulis (L.) and Arctica islandica (L.), Mar. Biol., 160, 2073-2087, 2013.

708
709 IPCC: Climate Change 2001: The Scientific Basis. Third Assessment Report of the Intergovernmental
710 Panel on Climate Change., Cambridge University Press, New York, USA. 82pp, 2001.

711
712 IPCC: Climate Change 2013: The Physical Science Basis. Working Group I Contribution to the Fifth
713 Assessment Report of the Intergovernmental Panel on Climate Change, Cambridge University Press,
714 New York, USA. 1435pp, 2013.

715
716 Jeffrey, S. W. and Welschmeyer, N. A.: Spectrophotometric and fluorometric equations in common use
717 in oceanography. In: Phytoplankton pigments in oceanography. , Jeffrey, S. W., Mantoura, R. F. C., and
718 Wright, S. W. (Eds.), UNESCO Publishing, Paris, 1997.

719
720 Johnes, P. and Heathwaite, A. L.: A procedure for the simultaneous determination of total nitrogen and
721 total phosphorus in freshwater samples using persulfate microwave digestion., Water Res., 26, 1281-
722 1287, 1992.

723
724 Karl, D. M.: Phosphorus, the staff of live, Nature, 406, 31-33, 2000.

725
726 Karl, D. M. and Bailiff, M. D.: The measurements of dissolved nucleotides in aquatic environments,
727 Limnol. Oceanogr., 34, 543-558, 1989.

728
729 Karl, D. M. and Björkman, K. M.: Dynamics of DOP. In: Biogeochemistry of marine dissolved organic
730 matter., Hansell, D. A. and Carlson, C. A. (Eds.), Academic Press, Amsterdam 2002.

731
732 Lass, H. U., Mohrholz, V., Nausch, G., and Siegel, H.: On phosphate pumping into the surface layer of the
733 eastern Gotland Basin by upwelling, J. Mar. Syst., 80, 71-89, 2010.

734

735 Llebot, C., Spitz, Y. H., Sole, J., and Estrada, M.: The role of inorganic nutrients and dissolved organic
736 phosphorus in the phytoplankton dynamics of a Mediterranean bay A modeling study, J. Mar. Syst., 83,
737 192-209, 2010.

738
739 Lomas, M. W., Burke, A. L., Lomas, D. A., Bell, D. W., Shen, C., Dyhrman, S. T., and Ammerman, J. W.:
740 Sargasso Sea phosphorus biogeochemistry: an important role for dissolved organic phosphorus (DOP),
741 Biogeosciences, 7, 695-710, 2010.

742
743
744 Lueker, T. J., Dickson, A. G., and Keeling, C. D.: Ocean pCO(2) calculated from dissolved inorganic carbon,
745 alkalinity, and equations for K-1 and K-2: validation based on laboratory measurements of CO2 in gas
746 and seawater at equilibrium, Mar. Chem., 70, 105-119, 2000.

747
748 MacGilchrist, G. A., Shi, T., Tyrrell, T., Richier, S., Moore, C. M., Dumousseaud, C., and Achterberg, E. P.:
749 Effect of enhanced pCO(2) levels on the production of dissolved organic carbon and transparent
750 exopolymer particles in short-term bioassay experiments, Biogeosciences, 11, 3695-3706, 2014.

751
752 Mehrbach, C., Culberson, C. H., Hawly, J. E., Pytkowicz, R., and M., D. J.: Measurement of the apparent
753 dissociation constats of carbonic acid in seawater at atmospheric pressure, Limnol. Oceanogr., 18, 897-
754 907, 1973.

755
756 Morris, A. W. and Riley, J. P.: The determination of nitrate in sea water, Anyl. Chim. Acta, 29, 272-279,
757 1963.

758
759 Murphy, J. and Riley, J. P.: A modified single solutionmethod for the determination of phosphate in
760 natural waters, Anyl. Chim. Acta, 27, 31-36, 1962.

761
762 Nausch, M. and Nausch, G.: Dissolved phosphorus in the Baltic Sea - Occurrence and relevance, J. Mar.
763 Syst., 87, 37-46, 2011.

764
765 Nausch, M., Nausch, G., Lass, H. U., Mohrholz, V., Nagel, K., Siegel, H., and Wasmund, N.: Phosphorus
766 input by upwelling in the eastern Gotland Basin (Baltic Sea) in summer and its effects on filamentous
767 cyanobacteria, Estuar. Coast. Shelf Sci., 83, 434-442, 2009.

768
769 Nausch, M., Nausch, G., Mohrholz, V., Siegel, H., and Wasmund, N.: Is growth of filamentous
770 cyanobacteria supported by phosphate uptake below the thermocline?, Estuar. Coast. Shelf Sci., 99, 50-
771 60, 2012.

772
773 Orr, J. C.: Recent and future changes in ocean carbonate chemistry. In: Ocean Acidification, Guttaso, J. P.
774 and Hansson, L. (Eds.), Oxford University Press, New York, 2011.

775
776 Pajusalu, L., Martin, G., and Pollumae, A.: Results of laboratory and field experiments of the direct effect
777 of increasing CO2 on net primary production of macroalgal species in brackish-water ecosystems, P. Est.
778 Acad. Sci., 62, 148-154, 2013.

Pansch, C., Nasrolahi, A., Appelhans, Y. S., and Wahl, M.: Impacts of ocean warming and acidification on the larval development of the barnacle Amphibalanus improvisus, J. Exp. Mar. Biol. Ecol., 420, 48-55, 2012.

Patey, M. D., Rijkenberg, M. J. A., Statham, P. J., Stinchcombe, M. C., Achterberg, E. P., and Mowlem, M.: Determination of nitrate and phosphate in seawater at nanomolar concentrations, Trac-Trends Anal. Chem., 27, 169-182, 2008.

Paul, A., Achterberg, E., Ouriqua, J., Bach, L., Schulz, K., Boxhammer, T., Czerny, J., Trense, Y., and Riebesell, U.: No measurable effect of ocean acidification on nitrogen biogeochemistry in a summer Baltic Sea plankton community, Biogeochemistry, submitted, 2015a.

Paul, A. J., Bach, L. T., Schulz, K.-G., Boxhammer, T., Czerny, J., Achterberg, E. P., Hellemann, D., Trense, Y., Nausch, M., Sswat, M., and Riebesell, U.: Effect of elevated CO2 on organic matter pools and fluxes in a summer, post spring-bloom Baltic Sea plankton community, Biogeosciences, 12, 6181-6203, 2015b.

Riebesell, U., Bellerby, R. G. J., Grossart, H. P., and Thingstad, F.: Mesocosm CO2 perturbation studies: from organism to community level, Biogeosciences, 5, 1157-1164, 2008.

Riebesell, U., Czerny, J., von Brockel, K., Boxhammer, T., Budenbender, J., Deckelnick, M., Fischer, M., Hoffmann, D., Krug, S. A., Lentz, U., Ludwig, A., Muche, R., and Schulz, K. G.: Technical Note: A mobile sea-going mesocosm system - new opportunities for ocean change research, Biogeosciences, 10, 1835-1847, 2013.

Riebesell, U. and Tortell, P.: Effects mof ocean acidification on pelagic organisms and ecosystems. In: Ocean acidification, Gattuso, J. P. and Hansson, L. (Eds.), Oxford Universitiy Press, New York, 2011.

Rossoll, D., Sommer, U., and Winder, M.: Community interactions dampen acidification effects in a coastal plankton system, Mar. Ecol.-Prog. Ser., 486, 37-46, 2013.

Sanudo-Wilhelmy, S. A., Kustka, A. B., Gobler, C. J., Hutchins, D. A., Yang, M., Lwiza, K., Burns, J., Capone, D. G., Raven, J. A., and Carpenter, E. J.: Phosphorus limitation of nitrogen fixation by Trichodesmium in the central Atlantic Ocean, Nature, 411, 66-69, 2001.

Schulz, K. G. and Riebesell, U.: Diurnal changes in seawater carbonate chemistry speciation at increasing atmospheric carbon dioxide, Mar. Biol., 160, 1889-1899, 2013.

Schulz, K. G., Riebesell, U., Bellerby, R. G. J., Biswas, H., Meyerhofer, M., Muller, M. N., Egge, J. K., Nejstgaard, J. C., Neill, C., Wohlers, J., and Zollner, E.: Build-up and decline of organic matter during PeECE III, Biogeosciences, 5, 707-718, 2008.

Siegel, H. and Gerth, M.: Sea surface temperature in the Baltic Sea in 2012. In: HELCOM Baltic Sea environment fact sheets, http://www.hwlcom.fi/baltic-sea-trends/environment-fact-sheet, 2013.

Simon, M. and Azam, F.: Protein content and protein synthesis rates of planktonic marine bacteria, Mar. Ecol.-Prog. Ser., 51, 201-213, 1989.

Simon, M. and Rosenstock, B.: Carbon and nitrogen sources of planktonic bacteria in Lake Constance studies by the composition and isotope dilution of intracellular amino acids., Limnol. Oceanogr., 37, 1496-1511, 1992.

Sc, W. and Chrost, R. J.: Utilization of selected dissolved organic phosphorus compounds by bacteria in lake water under non-limiting orthophosphate conditions, Pol. J. Environ. Stud., 10, 475-483, 2001.

Stemmer, K., Nehrke, G., and Brey, T.: Elevated CO2 Levels do not Affect the Shell Structure of the Bivalve Arctica islandica from the Western Baltic, PLoS ONE, 8, 2013.

Sugie, K. and Yoshimura, T.: Effects of pCO2 and iron on the elemental composition and cell geometry of the marine diatom Pseudo-nitzschia pseudodelicatissima (Bacillariophyceae), J. Phycol., 49, 475-488, 2013.

Sun, J., Hutchins, D. A., Feng, Y. Y., Seubert, E. L., Caron, D. A., and Fu, F. X.: Effects of changing pCO(2) and phosphate availability on domoic acid production and physiology of the marine harmful bloom diatom Pseudo-nitzschia multiseries, Limnol. Oceanogr., 56, 829-840, 2011.

Suzumura, M. and Ingall, E. D.: Concentrations of lipid phosphorus and its abundance in dissolved and particulate organic phosphorus in coastal aeawater, Mar. Chemistry, 75, 141-149, 2001.

Suzumura, M. and Ingall, E. D.: Distribution and dynamics of various forms of phosphorus in seawater: insight from field observation in the Pacific Ocean an a laboratory experiment, Deep-Sea Res. Part I-Oceanogr. Res. Pap., 51, 1113-1130, 2004.

Tanaka, T., Thingstad, T. F., Lovdal, T., Grossart, H. P., Larsen, A., Allgaier, M., Meyerhofer, M., Schulz, K. G., Wohlers, J., Zollner, E., and Riebesell, U.: Availability of phosphate for phytoplankton and bacteria and of glucose for bacteria at different pCO(2) levels in a mesocosm study, Biogeosciences, 5, 669-678, 2008.

Tyrrell, T.: The relative influences of nitrogen and phosphorus on oceanic primary production, Nature, 400, 525-531, 1999.

Unger, J., Endres, E., Wannicke, N., Engel, A., Voss, M., Nausch, G., and Nausch, M.: Response of Nodularia spumigena to pCO2 – Part 3: Turnover of phosphorus compounds, Biogeosciences, 10, 1483-1499, 2013.

Vehmaa, A., Brutemark, A., and Engstrom-Ost, J.: Maternal Effects May Act as an Adaptation Mechanism for Copepods Facing pH and Temperature Changes, PLoS ONE, 7, 2012.

Wannicke, N., Endres, S., Engel, A., Grossart, H. P., Nausch, M., Unger, J., and Voss, M.: Response of Nodularia spumigena to pCO(2) - Part 1: Growth, production and nitrogen cycling, Biogeosciences, 9, 2973-2988, 2012.

Yoshimura, T., Sugie, K., Endo, H., Suzuki, K., Nishioka, J., and Ono, T.: Organic matter production response to CO2 increase in open subarctic plankton communities: Comparison of six microcosm experiments under iron-limited and -enriched bloom conditions, Deep-Sea Res. Part I-Oceanogr. Res. Pap., 94, 1-14, 2014.

Tables and figures

Table 1: Minimum, maximum and mean values of hydrographical parameters and fCO_2 for the different phases in the fjord. Temperatures in the mesocosms were identical with those in surrounding fjord water.

phase	min	max	mean
	water temperature (°C)		
0	7.82	8.71	8.20
I	9.66	15.86	12.27
II	7.89	14.79	11.68
III	8.35	12.61	10.83
	salinity		
0	5.72	5.85	5.78
I	5.46	5.85	5.65
II	5.67	6.04	5.82
III	5.9	6.05	5.98
	pH		
0	8.09	8.23	8.16
I	8.11	8.30	8.17
II	7.81	8.30	8.00
III	7.75	7.93	7.83
	fCO_2 (µatm)		
0	250	347	298
I	207	336	283
II	208	679	465
III	521	800	668

Table 2: Mesocosms in which the Spearman Rank correlation between P-pools or uptake rates and other parameters was significant. The relationship of PP with TP and Chl*a* was significant only in the untreated mesocosms while the correlation to PC was also significant in the mesocosms with intermediate CO_2 levels. DOP was related to temperature only in the high CO_2 treatments. Under high fCO_2 conditions, the PO_4 uptake in the size fraction >3µm correlated with Chl_a and the P content of phytoplankton.

Relationship between	***f*CO$_2$ (µatm)**	**significant responses** r	p	n
PP-TP	365	0.599	0.008	18
	368	0.515	0.029	18
PP - Chl*a*	365	0.479	0.0130	25
	368	0.584	0.0022	25
PO_4 - Chl*a*	365	-0.832	<0.0001	21
	368	-0.756	0.0011	20
	497	-0.674	0.0008	21
	821	-0.524	0.0147	21
	1007	-0.634	0.0027	20
PP -PC	365	0.542	0.0061	24
	368	0.625	0.0011	24
	497	0.404	0.0490	24
	821	0.551	0.0052	24
DOP -temperature	1007	0.488	0.0470	17
	1231	0.525	0.0310	17
PO_4 uptake>3µm - Chl*a*	497	0.743	0.0056	12
	821	0.674	0.0081	14
	1231	0.476	0.0310	14
PO_4 uptake>3µm - POP/Chl*a*	497	-0.601	0.0380	12
	821	-0.631	0.0160	14
	1231	-0.626	0.0165	14

Table 3: Contribution of different phosphorus components to DOP in the mesocosms and in the fjord.

fCO_2	contribution to DOP (%)					
(µatm)	ATP-P	PL-P	DNA-P	RNA-P	sum	unidentified P
Fjord	0.7	0.7	0.04	69.4	70.84	29.16
365	0.7	0.5	0.03	44.1	45.33	54.67
368	0.6	0.5	0.03	46.9	48.03	51.97
497	0.6	0.4	0.04	49.5	50.54	49.46
821	0.6	0.4	0.03	41.8	42.83	57.17
1003	0.8	0.4	0.04	60.1	61.34	38.66
1231	0.5	0.4	0.03	48.6	49.53	50.47

Table 4: PO_4- and ATP uptake rates in the fjord and in the mesocosms. Minimum, maximum and mean values as well as the contribution of the size fraction <3 µm to the total activity are given for the whole period of investigation (each: n= 16 for PO_4 and n=6 for ATP uptake).

fCO_2	total PO_4 uptake ($nmol l^{-1} h^{-1}$)			portion (%)	total ATP-P uptake ($nmol l^{-1} h^{-1}$)			portion (%)
	min	max	mean	<3µm	min	max	mean	<3µm
Fjord	0.87	2.81	1.63 ± 0.58	76 ± 15	0.04	0.51	0.26 ± 0.15	92 ± 5
365	0.82	3.89	1.67 ± 0.82	81 ± 11	0.14	1.08	0.43 ± 0.33	96 ± 2
368	0.65	2.74	1.61 ± 0.58	86 ± 7	0.16	0.97	0.47 ± 0.27	96 ± 2
497	0.61	3.03	1.52 ± 0.59	86 ± 6	0.20	1.07	0.54 ± 0.28	96 ± 2
821	0.91	2.83	1.60 ± 0.59	88 ± 8	0.14	0.71	0.36 ± 0.21	97 ± 2
1003	0.67	3.79	1.73 ± 0.85	86 ± 6	0.22	0.69	0.39 ± 0.15	97 ± 1
1231	0.87	2.23	1.53 ± 0.43	87 ± 6	0.17	0.67	0.44 ± 0.17	97 ± 2

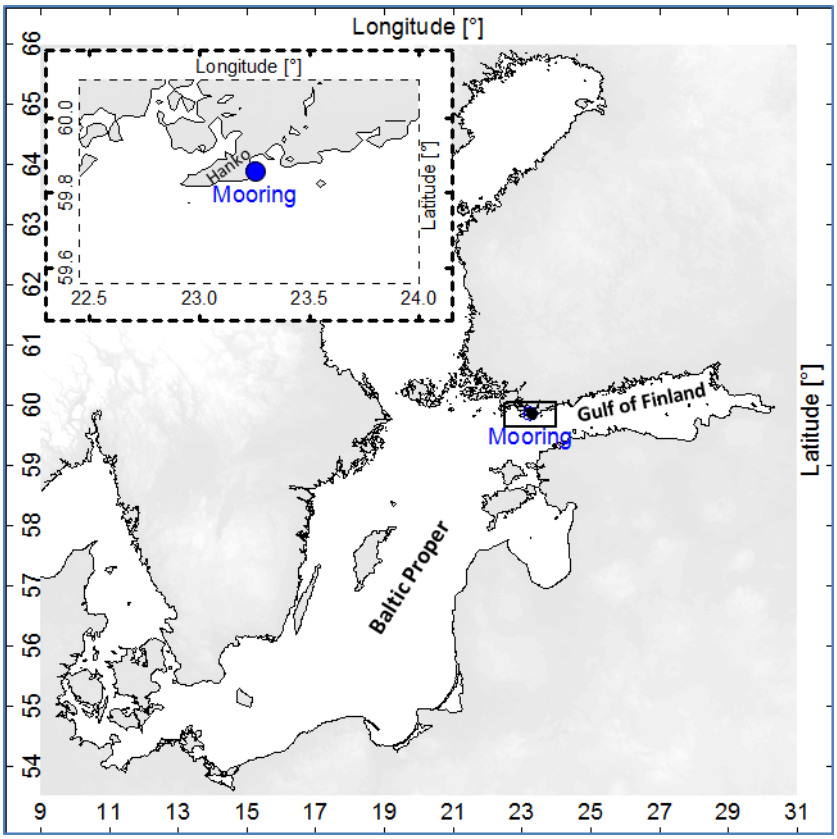

Figure 1: The Baltic Sea and the location near the peninsula Hanko in the western Gulf of Finland where the mesocosms were deployed

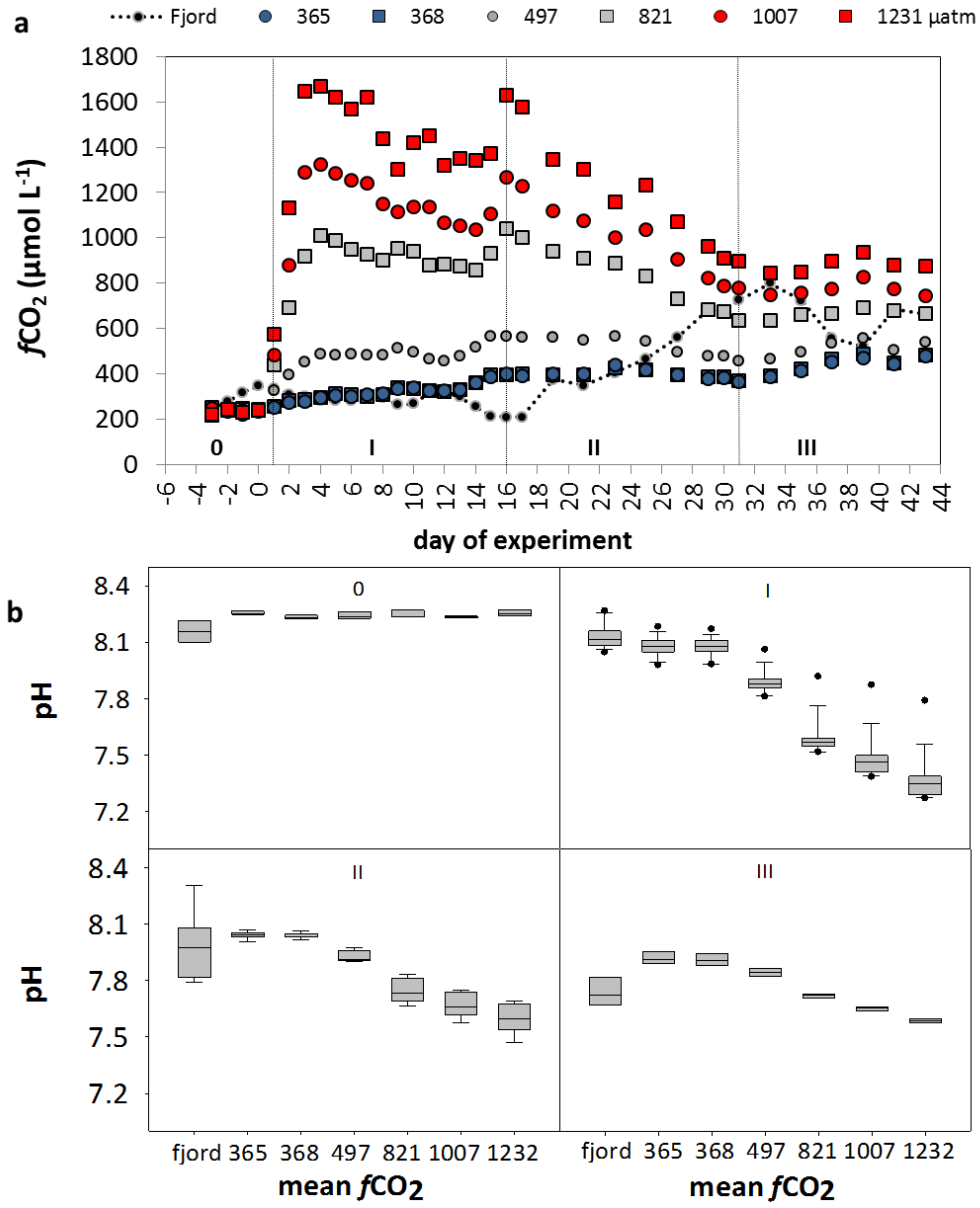

Figure 2a: fCO_2 values in the mesocosms and in the fjord throughout the experiment. Small black dots show the fCO_2 in the ambient fjord water. Treatment of the mesocosms with CO_2 saturated fjord water at the beginning of the experiment (days 0-4) created different fCO_2 levels in the mesocosms: blue symbols represents the untreated mesocosms, grey the intermediate, and red the high CO_2 treated mesocosms. The treatment was repeated at day 16.
Figure 2b: Corresponding pH ranges in the mesocosms during the four phases. Despite decreasing trend over time, a gradient between the mesocosms was kept over the whole period.

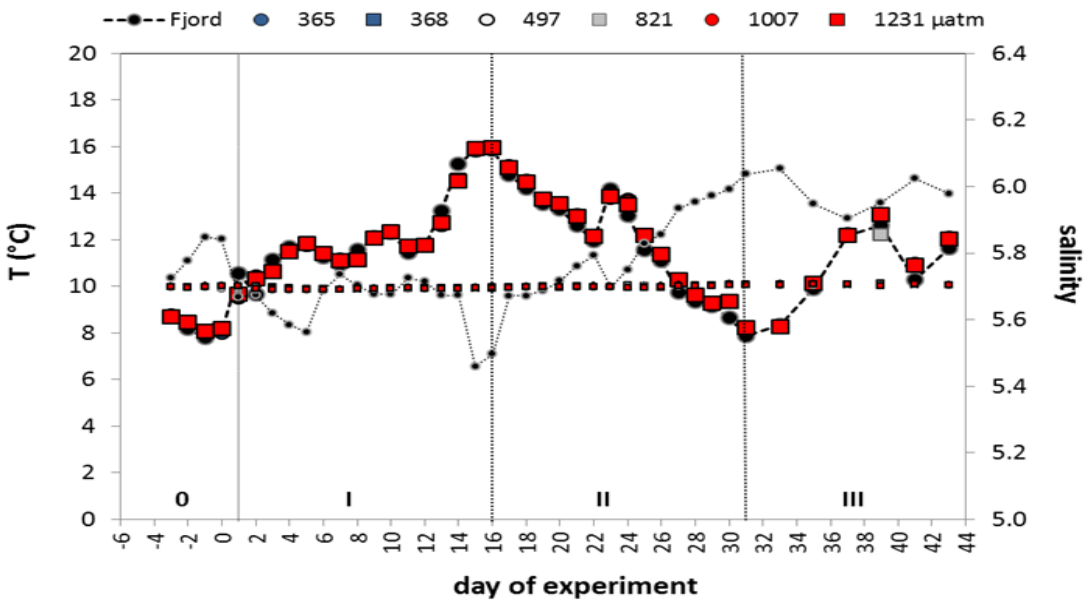

Figure 3: Temperature and salinity averaged over the 17 m surface layer of the mesocosms and the fjord. The data were obtained from daily CTD casts. Large symbols represent temperature and the small symbols salinity. Fjord water is shown as black dots with broken line while blue symbols denote untreated, grey intermediate and red high fCO_2 levels in the mesocosms. According to the temperature regime, the experimental period can be divided into four phases (phases 0, I, II and III).

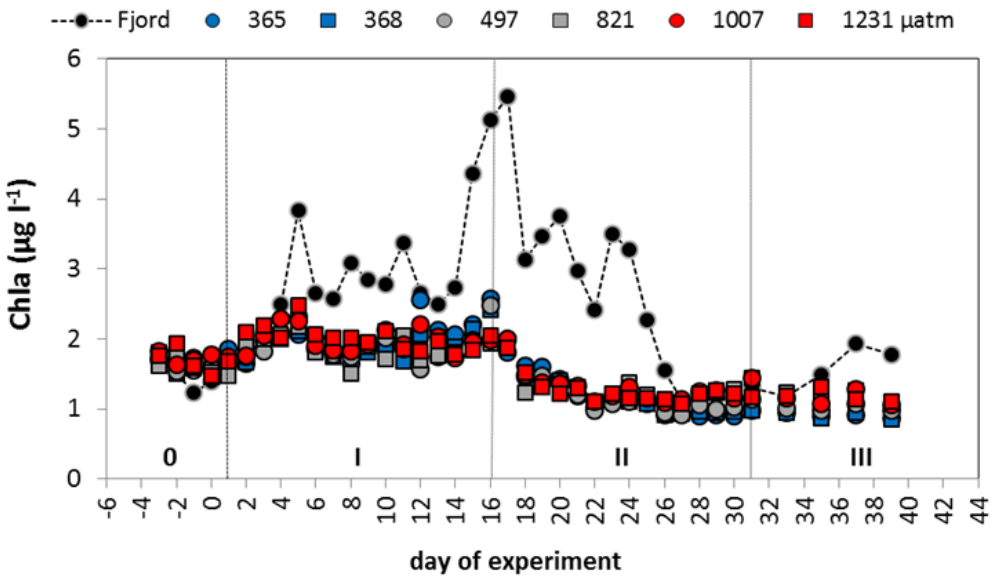

Figure 4: Chl*a* concentrations in fjord water and in the mesocosms with different fCO_2 conditions. The development over time can be divided into three phases as well. Blue represent untreated, grey intermediate, and red highly treated fCO_2 levels. Black dots with dotted line are the Chl*a* concentrations in the fjord water.

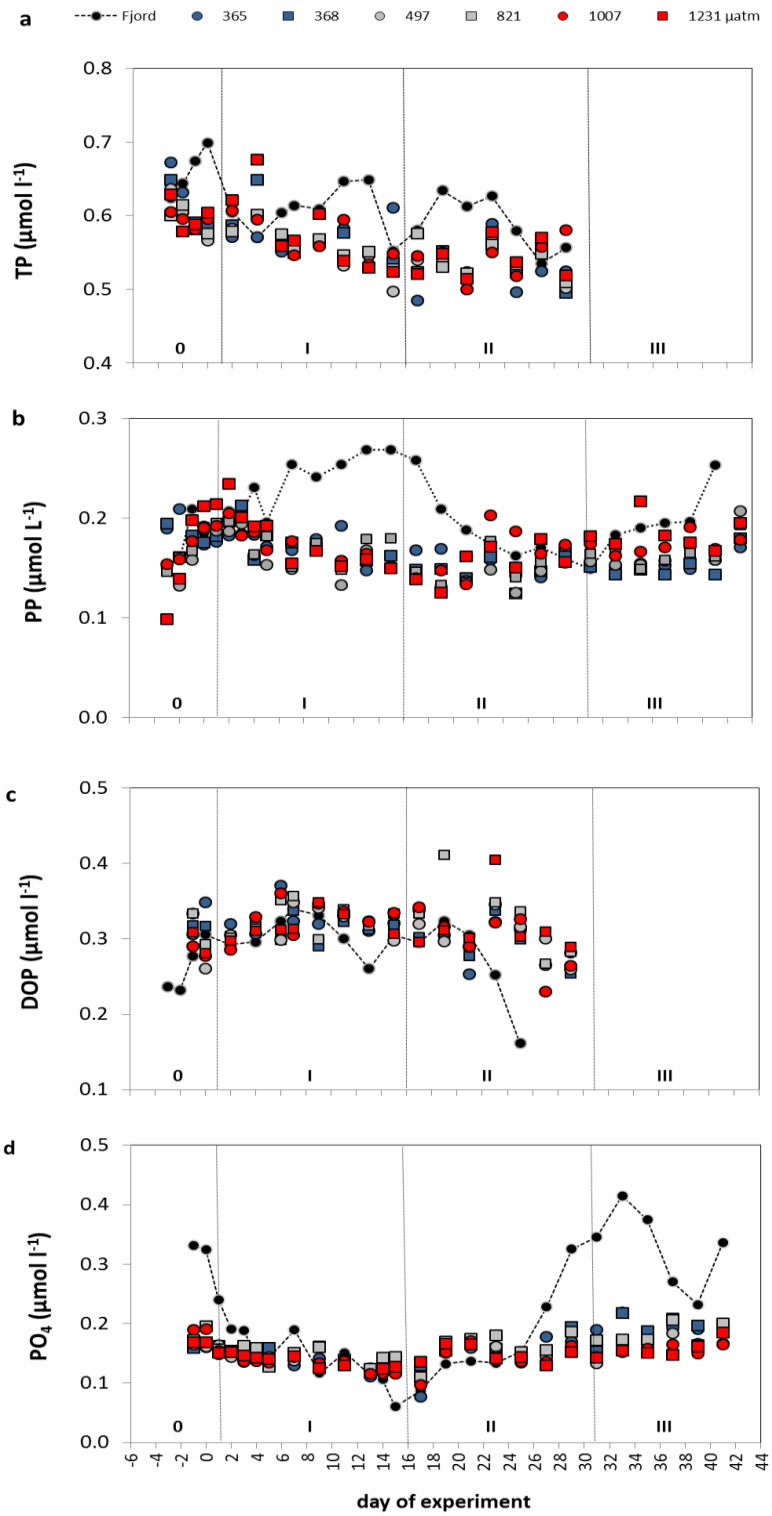

Figure 5a-d: Development of total phosphorus (TP) and the three measured P-fractions in fjord water (black dots with dotted line) and in the mesocosms over time. Blue represents untreated, grey intermediate and red high fCO_2 treatment levels.

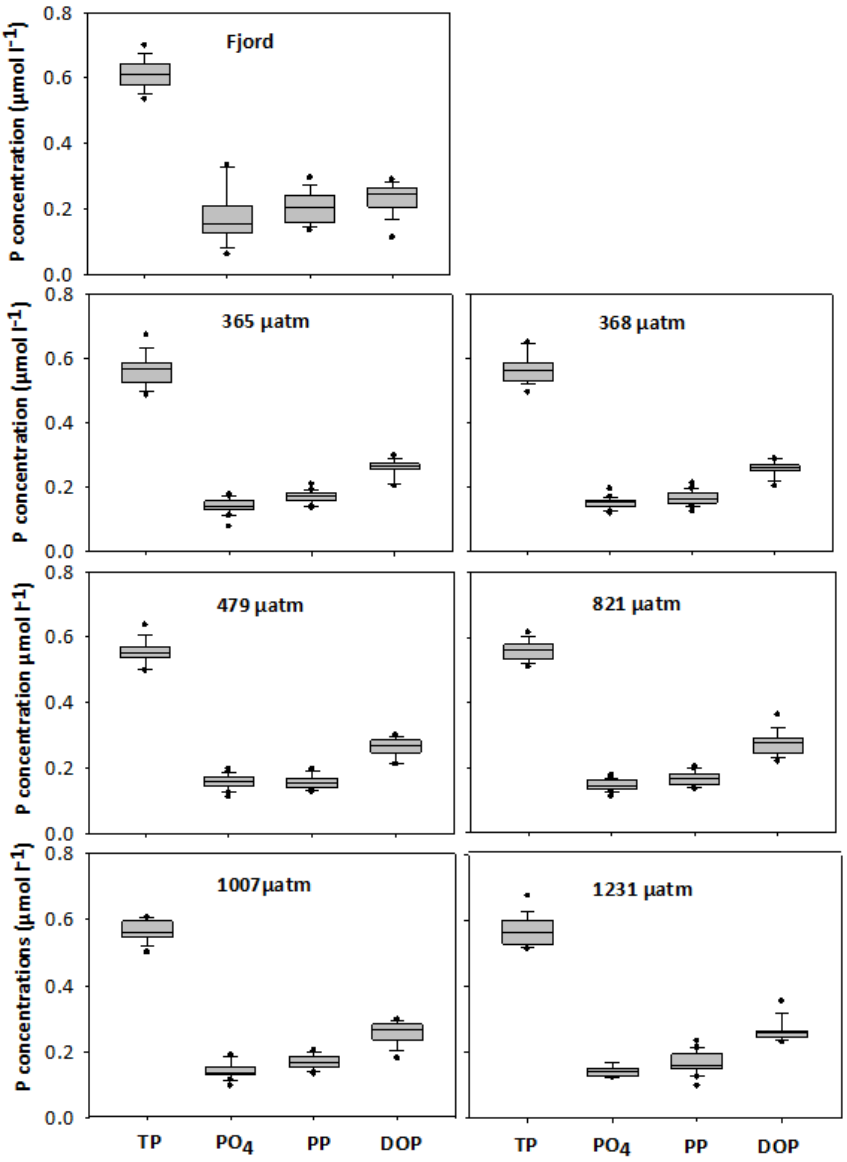

Figure 6: Contribution of the individual P-fractions to TP in fjord water and in the respective mesocosms. The data are averaged for the period when TP measurements were done (day -3 – day 29).

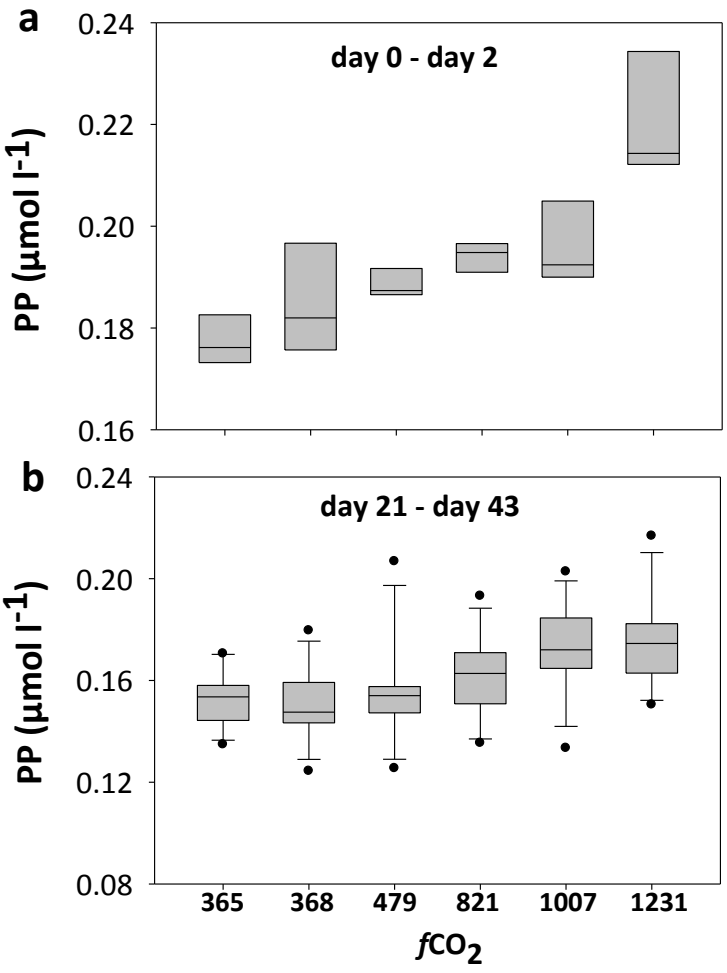

Figure 7: PP concentration in the mesocosms during the initial phase from day 0 to day 2 (a) and from day 23 until the end (b) of experiment.

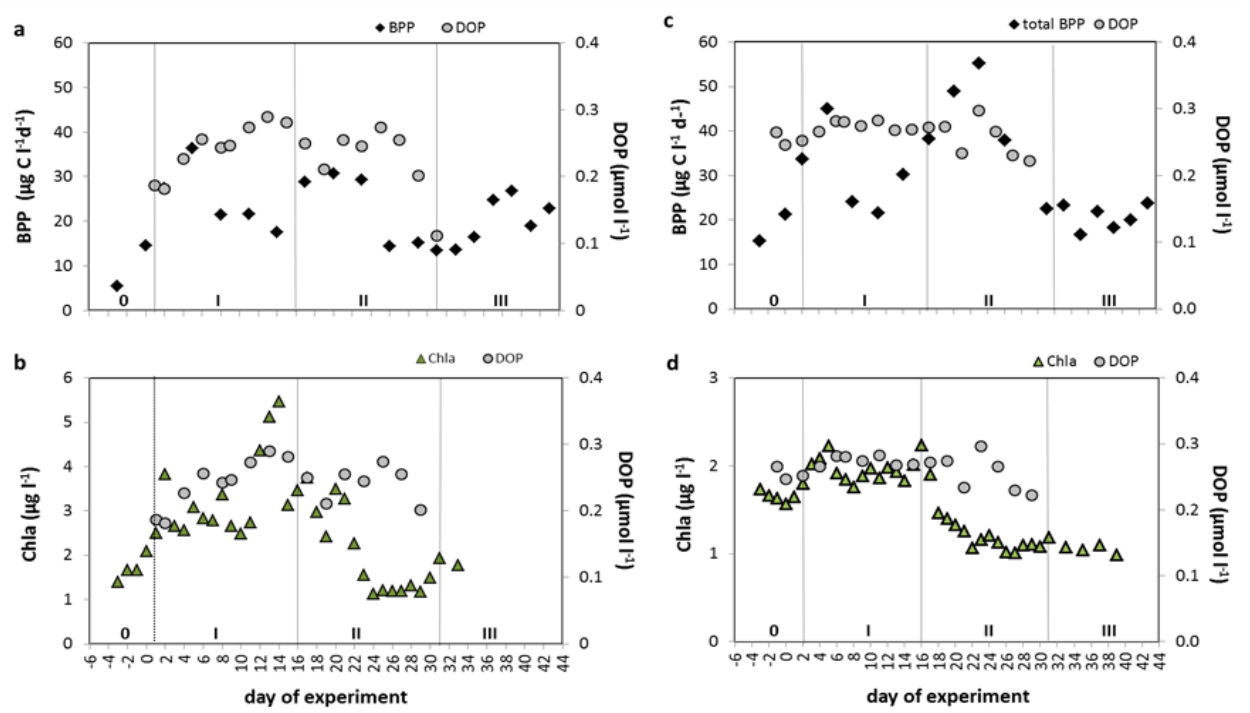

Figure 8: Development of DOP in relation to bacterial production (BPP) and phytoplankton biomass (Chl*a*) in the fjord (a, b) and in the mesocosms (c, d). For mesocosms, mean values averaged over all treatments are given.

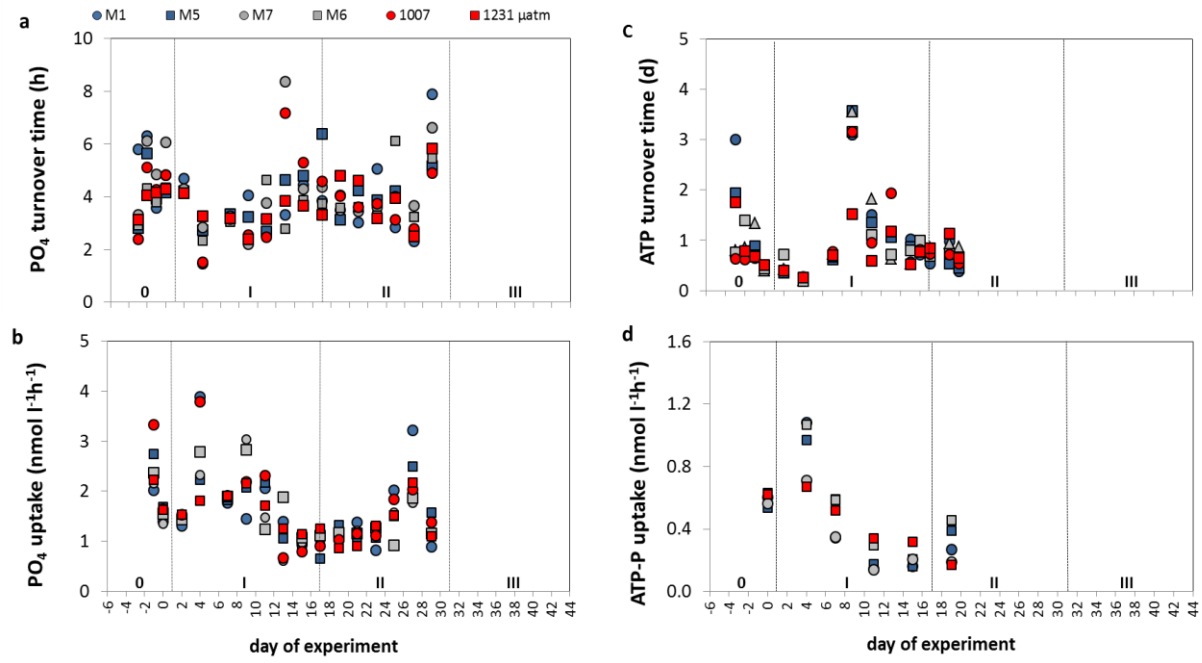

Figure 9: Turnover times of PO_4 (a) and ATP (c) in the mesocosms as well as the respective uptake rates (b, d).

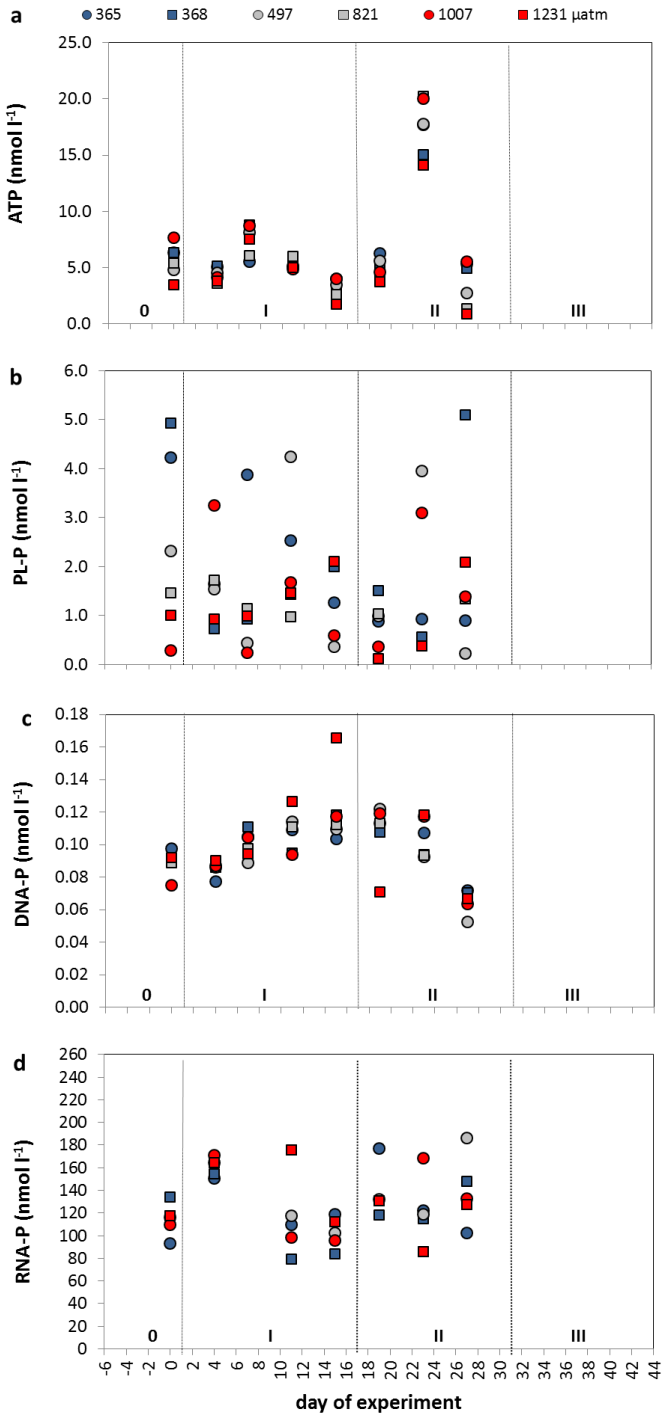

Figure 10: Development of DOP compounds in the mesocosms and in the fjord from day 0 to day 27.